COMPARISON OF InGaAs ABSORPTIVE GRATING STRUCTURES IN 1.55μm InGaAsP/InP STRAINED MQW GAIN-COUPLED DFB LASERS

Masaki Funabashi, Hidekazu Kawanishi, Tsurugi K. Sudoh, Toru Nakura,
Dietmar Schmitz†, Frank Schulte†, Yoshiaki Nakano, and Kunio Tada

Department of Electronic Engineering, University of Tokyo
7-3-1 Hongo, Bunkyo-ku, Tokyo, 113, Japan
†AIXTRON Semiconductor Technologies GmbH, D-52072 Aachen, Germany

Abstract

In gain-coupled (GC) distributed-feedback (DFB) lasers of absorptive grating type, the device characteristics depend very much on the absorptive grating configuration such as duty cycle, layer thickness, conduction type, and material composition. We have fabricated 1.55μm InGaAsP/InP strained multiple quantum well (MQW) DFB lasers having different absorptive grating thickness and different conduction type. Lasing characteristics of these lasers were compared in view of coupling coefficients and absorption saturation. Through net gain measurement, information useful for designing and optimizing the absorptive grating was obtained.

I. Introduction

Gain-coupled DFB lasers have many advantages over conventional index-coupled (IC) DFB lasers such as high longitudinal single-mode yield [1], immunity to facet reflection [2]. Furthermore, these advantages can be obtained without using complicated phase-shifting structures like quarter wave phase shift or multiple phase shift.

In GC DFB lasers of absorptive grating type, the device characteristics depend very much on the absorptive grating configuration such as duty cycle, layer thickness, conduction type, and material composition. However, guideline for designing or optimizing absorptive grating has not been established. This is partly because there has been no easy and reliable method to evaluate coupling coefficients of DFB lasers precisely. Recently, automatic laser parameter extraction from subthreshold spectra has been made possible. It is applicable to both index- and gain-coupled DFB lasers even without facet anti-reflection (AR) coating. By using this method, most of DFB laser parameters such as coupling coefficients, grating phases at facets, effective refractive index, and its wavelength dispersion can be determined simultaneously [3, 4].

We have fabricated 1.55 μm InGaAsP/InP strained multiple quantum well (MQW) DFB lasers having different absorptive grating thickness and conduction type. Since some of the laser parameters might vary above threshold, we demonstrate net gain measurement in order to understand how the absorptive grating behaves with output optical power. Then, we compare lasing characteristics of these lasers in view of coupling coefficients and absorption saturation in the absorptive grating.

II. Device Structure and Fabrication

Figures 1 and 2 illustrate the bird's-eye view and the

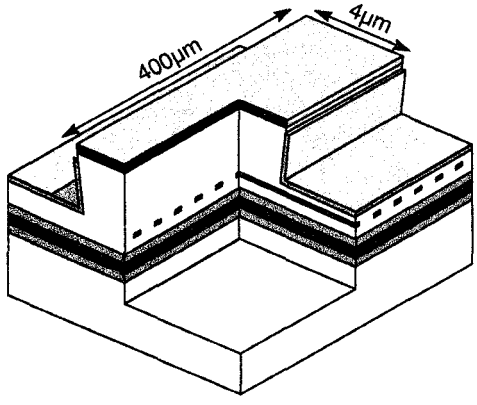

Fig. 1. Schematic drawing of the ridge-waveguide absorptive-grating gain-coupled DFB laser.

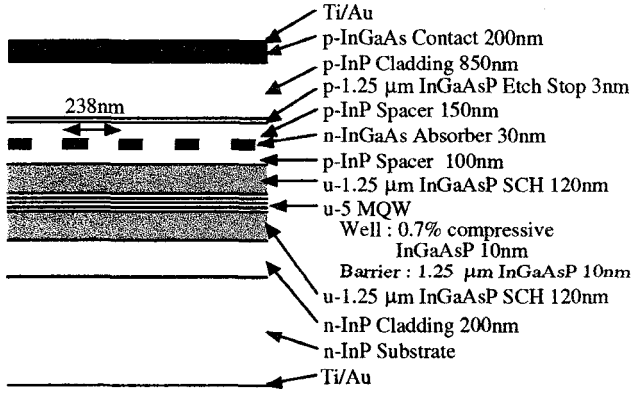

Fig. 2. Schematic longitudinal cross-section of the gain-coupled DFB laser with 30nm-thick n-InGaAs absorptive grating.

0-7803-3898-7/97/$10.00 ©1997 IEEE

longitudinal cross section of the laser structure. The layers were grown by two-step metal-organic vapor phase epitaxy (MOVPE, AIX200/4) with TBP and TBAs as group V precursors. The growth temperature was 610°C and the pressure was 10kPa. The doping levels of the cladding, absorptive, and contact layers were about $5x10^{17}$ (Zn and S), $5x10^{17}$ (Zn or S), $1x10^{19}$ (Zn) cm^{-3}, respectively. The active layer is composed of five compressively strained (0.7%) InGaAsP wells and 1.25 μm barriers (10 nm thick each). The absorptive grating with 238 nm period was formed by holographic exposure and wet chemical etching of the InGaAs layer. Here, two different values were used for the thickness of the InGaAs absorptive grating, namely, 10 nm and 30 nm. For 30nm-thick absorber, both p-doped and n-doped InGaAs were tried whereas the 10nm InGaAs was undoped. Duty cycle of the grating was ~30 %. After the second step MOVPE on the grating, the wafer was made into ridge waveguide configuration (400 μm-long and 4μm-wide) by utilizing the 3 nm-thick quaternary etch stop layer. For the sake of comparison, conventional index-coupled DFB lasers were fabricated at the same time. Facets of the lasers were left as-cleaved. Laser chips were bonded on heatsinks with tin solder.

III. Characteristics

Typical cw threshold currents at 20°C were 18, 20, and 25 mA for IC and GC with 10 and 30 nm-thick gratings, respectively. Slight threshold increase is attributed to excess absorption by the grating. Index and gain coupling coefficients, κ_i and κ_g, were extracted from subthreshold spectra [3, 4]. Figure 3 shows a typical fitting result in the GC DFB laser with the 30nm-thick n-InGaAs absorber. Measured and calculated spectra are almost completely matched, and extracted κ_i and κ_g of this laser are $62cm^{-1}$ and $-13cm^{-1}$, respectively.

Bias dependence of index- and gain-coupling coefficients in different grating configurations are plotted in Figs. 4 (a) and (b). Since both real and imaginary parts of the refractive index of the InGaAs absorptive grating are different from those of surrounding InP, not only gain coupling but also index coupling is incorporated. The 30 nm-thick grating resulted in larger κ_i and κ_g (the minus sign of κ_g corresponds to loss coupling), which is reasonable.

In order to investigate saturation behavior of the absorptive grating, we measured net gain in the laser cavity by Hakki-Paoli method [5]. From peak to valley ratio r in measured spectra, cavity length L, and facet power reflectivity R, one can calculate net gain g_{net} by following equation,

$$g_{net} \equiv \Gamma g_{mat} - a_{loss} = \frac{1}{L}\ln\frac{\sqrt{r}-1}{\sqrt{r}+1} + \frac{1}{L}\ln\frac{1}{R} \qquad (1)$$

where Γ is optical confinement factor into active layer, g_{mat} is material gain, and α_{loss} is waveguide loss. Though equation (1) is for a Fabry-Perot cavity, we may apply this formulation to DFB lasers if wavelength is apart from the Bragg wavelength. R was assumed to be 0.3. Figure 5 shows bias

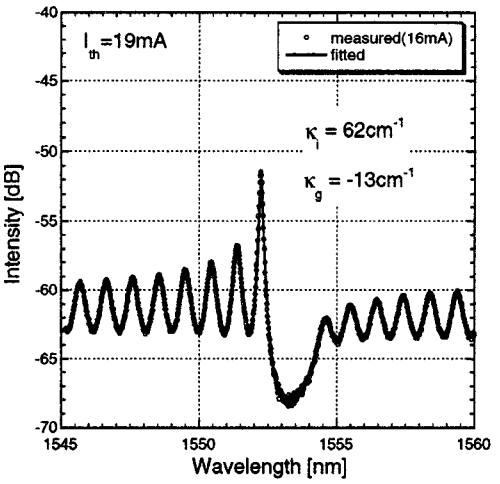

Fig. 3. Typical fitting result in the gain-coupled DFB LD with 30nm-thick n-InGaAs absorber.

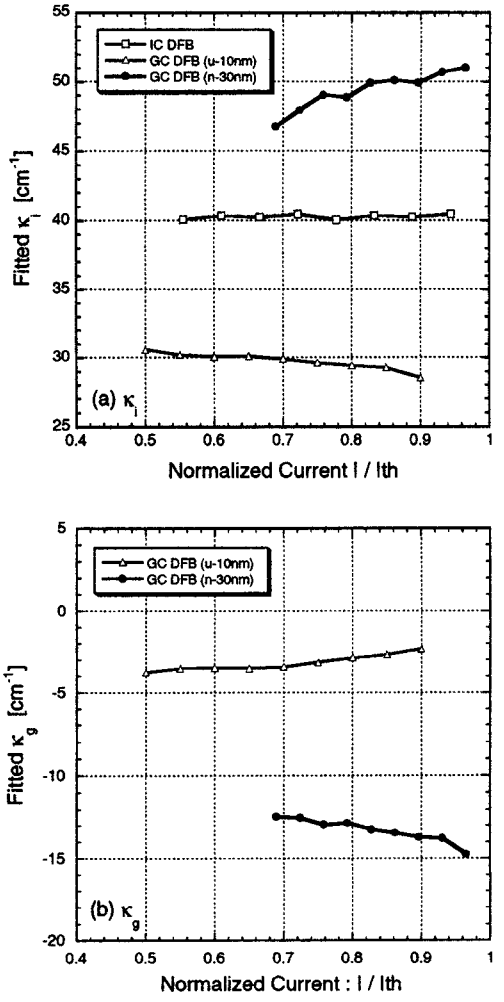

Fig. 4. Bias dependence of the index-coupling (a) and gain-coupling (b) coefficients extracted from subthreshold spectra.

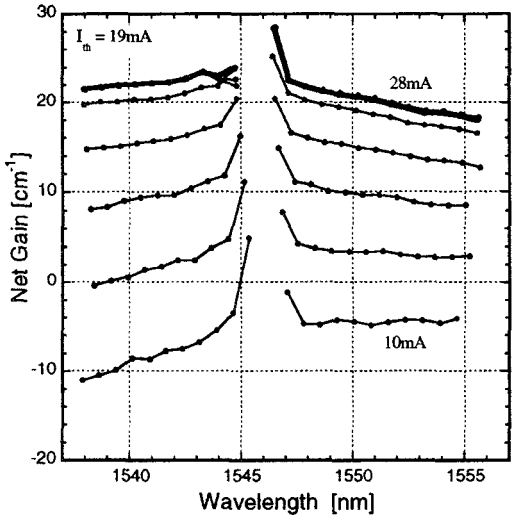

Fig. 5. Bias dependence of the net gain curve in the index-coupled DFB laser. Thick solid line represents threshold. Current step is 2mA.

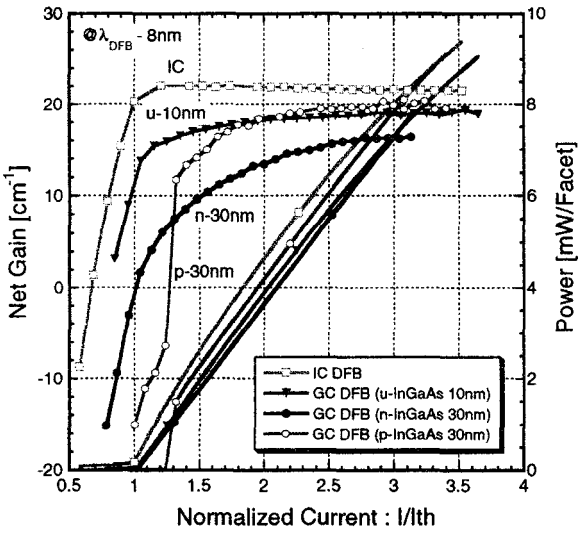

Fig. 7. Net gain and output power versus normalized injection current.

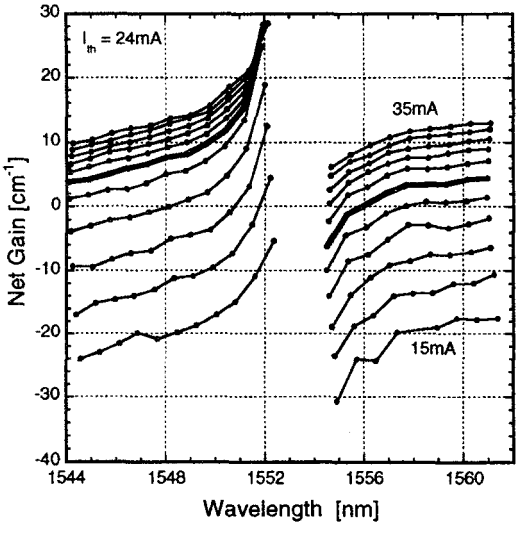

Fig. 6. Bias dependence of the net gain curve in the gain-coupled DFB laser with 30nm-thick n-InGaAs absorptive grating. Thick solid line represents threshold. Current step is 2mA.

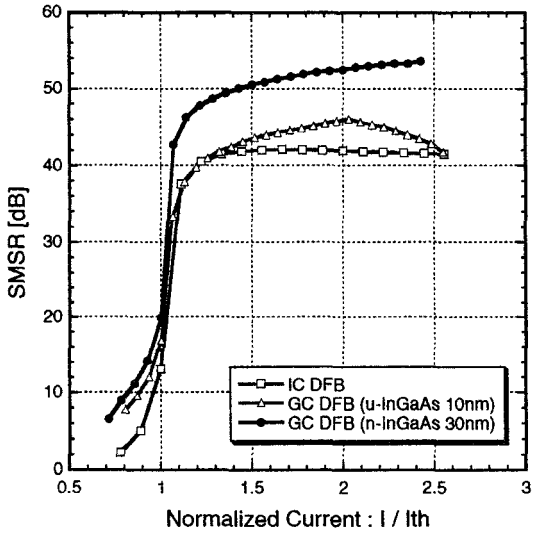

Fig. 8. Side mode suppression ratio versus normalized injection current.

dependence of the net gain curve in the index-coupled DFB laser. Due to the DFB modes, net gain cannot be evaluated correctly near the Bragg wavelength (around 1546nm in this laser). Thick solid line in the figure is at the threshold. Below threshold, net gain increases with bias current. However, when it reaches threshold, the gain stops increasing and remains constant. This is because carrier density in the active layer above threshold is fixed at the threshold value and therefore net gain is also unchanged.

In the GC DFB laser in Fig. 6, on the other hand, net gain continues increasing even above threshold. This difference could be explained as follows. In GC DFB lasers, the modes whose standing wave antinodes overlap with the grating are absorbed, and thus side modes are suppressed. Above threshold, the main mode of the cavity is intensified, and absorption begins to saturate. This absorption decrease results in net gain increase through the reduction of the waveguide loss.

The large net gain discontinuity across the DFB mode in Fig. 6 is attributed to the absorption coupling; the modes on

the longer wavelength side have their antinodes overlapping on the absorptive grating while the modes on the shorter wavelength side have nodes on the grating, thus being free from the absorption. Such discontinuity is not observed in the index-coupled DFB laser in Fig. 5 as expected.

To make a comparison among different absorptive grating configurations, net gains at a certain wavelength (λ_{DFB} - 8 nm) are plotted against normalized injection current in Fig. 7, together with L-I characteristics. Above threshold, the gain in the IC DFB laser is flat and completely fixed. On the other hand, in the GC DFB lasers, the gains keep increasing. This tendency is more notable in the GC DFB laser with thicker grating. In 10nm-thick absorber, amount of the net gain change is very small and absorption saturation begins earlier than that in 30nm-thick n-InGaAs absorber. However, in 30nm-thick p-InGaAs grating, it is found that absorption saturation occurs rapidly right after threshold. Nonlinear behavior due to this rapid absorption saturation can also be seen in the L-I curve, which is similar to what was reported before in GaAlAs/GaAs material system [6]. In order to prevent the absorption saturation at relatively low output power level, conduction-type-inverted thick absorptive grating is effective.

Because of the absorption compression observed in Fig. 7, κ_g above threshold might be reduced. Since the parameter extraction is only applicable to subthreshold spectra, κ_g above threshold cannot be evaluated by fitting. Instead, we measured side mode suppression ratio (SMSR) of the lasers, the result of which is shown in Fig. 8. In the 10nm-grating GC DFB laser, the SMSR begins to decrease at twice threshold. This means that the absorptive grating doesn't work any more and the laser becomes like an index-coupled DFB laser as the output power increases.

However, the SMSR of the 30 nm n-InGaAs GC DFB laser is not much affected since the bleaching is not substantial as in the case of the 10 nm absorber GC DFB laser.

The above information helps understanding how the absorptive grating works above threshold, and is useful for designing the grating configuration.

IV. Conclusion

We have fabricated 1.55μm strained MQW ridge waveguide gain-coupled DFB lasers having different absorptive grating configuration. Both gain- and index-coupling coefficients of the lasers were extracted and determined successfully from the subthreshold spectra. By means of Hakki-Paoli net gain measurement, we compared absorption saturation behavior for different absorptive grating thickness and conduction type. Utilizing this information, design and optimization of the absorptive grating having desired coupling coefficients and saturation behavior would be possible.

Acknowledgments

This work was supported by NEDO R&D Program #C300, the Mitsubishi Foundation, the Mombusho Grant-in-Aid #08555011 and #08044123.

References

[1] Y. Nakano, H. L. Cao, K. Tada, Y. Luo, M. Dobashi, and H. Hosomatsu, "Absorptive-grating gain-coupled distributed-feedback MQW lasers with low threshold current and high single-longitudinal-mode yield," Jpn. J. Appl. Phys., vol. 32, no. 2, pp. 825-829, February 1993.

[2] Y. Luo, Y. Nakano, and K. Tada, "Facet reflection independent, single longitudinal mode oscillation in a GaAlAs/GaAs distributed feedback laser equipped with a gain-coupling mechanism," Appl. Phys. Lett., vol. 55, no. 16, pp. 1606-1608, October 1989.

[3] G. Morthier, K. Sato, R. Baets, T. K. Sudoh, Y. Nakano, and K. Tada, "Parameter extraction from subthreshold spectra in cleaved gain- and index-coupled DFB LDs," Technical Digest, Conference on Optical Fiber Communication (OFC), FC3, pp. 309-310, San Diego, California, March 1995.

[4] T. Nakura, K Sato, M. Funabashi, G. Morthier, R. Baets, Y. Nakano, and K. Tada, "First observation of changing coupling coefficients in a gain-coupled DFB laser with absorptive grating by automatic parameter extraction from sub-threshold spectra," to be presented at the Conference on Lasers and Electro-Optics (CLEO), May 1997.

[5] B. W. Hakki and T. L. Paoli, "Gain spectra in GaAs double-heterostructure injection lasers," J. Appl. Phys., vol. 46, no. 3, pp. 1299-1306, March 1975.

[6] Y. Luo, H. L. Cao, M. Dobashi, H. Hosomatsu, Y. Nakano, K. Tada, "Gain-coupled distributed feedback semiconductor lasers with an absorptive conduction-type inverted grating," IEEE Photon. Technol. Lett., vol. 4, no. 7, pp. 692-695, July 1992.